JAAS

Accepted Manuscript

This is an *Accepted Manuscript*, which has been through the Royal Society of Chemistry peer review process and has been accepted for publication.

Accepted Manuscripts are published online shortly after acceptance, before technical editing, formatting and proof reading. Using this free service, authors can make their results available to the community, in citable form, before we publish the edited article. We will replace this *Accepted Manuscript* with the edited and formatted *Advance Article* as soon as it is available.

You can find more information about *Accepted Manuscripts* in the Information for Authors.

Please note that technical editing may introduce minor changes to the text and/or graphics, which may alter content. The journal's standard Terms & Conditions and the Ethical guidelines still apply. In no event shall the Royal Society of Chemistry be held responsible for any errors or omissions in this *Accepted Manuscript* or any consequences arising from the use of any information it contains.

ROYAL SOCIETY OF CHEMISTRY

www.rsc.org/jaas

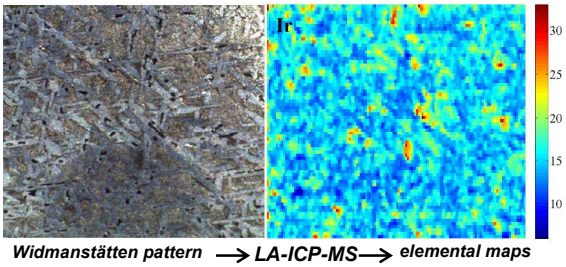

In this work, the capabilities and limitations of ns-LA-ICP-MS for bulk and spatially resolved (elemental mapping) analysis of iron meteorites were assessed.

Cite this: DOI: 10.1039/c0xx00000x

www.rsc.org/xxxxxx

ARTICLE TYPE

Evaluation of pneumatic nebulization and ns-laser ablation ICP-MS for bulk elemental analysis and 2- dimensional element mapping of iron meteorites

Stepan M. Chernonozhkin,[a] Steven Goderis,[a,b] Stephen Bauters,[a] Bart Vekemans,[a] Laszlo Vincze,[a] Philippe Claeys[b] and Frank Vanhaecke*[a]

Received (in XXX, XXX) Xth XXXXXXXXX 20XX, Accepted Xth XXXXXXXXX 20XX
DOI: 10.1039/b000000x

The capabilities and limitations of nanosecond laser ablation ICP – mass spectrometry for bulk and spatially resolved (elemental mapping) analysis of iron meteorites were assessed. The quantitative data obtained were compared to those obtained via multi-element solution ICP-MS (after digestion) relying on external calibration and high-accuracy determination of selected platinum group elements using solution ICP-MS after target element isolation using anion exchange chromatography and deploying isotope dilution. Results generated by the different methods described show good agreement. Significant matrix effects were observed to affect the results of the ns-LA-ICP-MS analysis of iron meteorites, making quantification via a matrix-matched standard a prerequisite. Careless use of intensity distribution maps without proper correction for laser-solid coupling efficiency can lead to incorrect interpretation of the element maps. ns-LA-ICP-MS was shown to be suitable for fast and quasi-nondestructive analysis of iron meteorites, not only homogeneous ataxites and hexahedrites, but also more heterogeneous ones, when considering ablated areas of a sufficient size. In the context of elemental mapping using LA-ICP-MS, Pearson's product-moment correlation analysis was demonstrated to be a powerful tool that can provide valuable information on the fractionation of the elements in the parent bodies of meteorites.

[a] *Ghent University, Department of Analytical Chemistry, Krijgslaan 281 – S12, 9000 Ghent, Belgium. E-mail: Frank.Vanhaecke@UGent.be*
[b] *Vrije Universiteit Brussel, Earth System Sciences, Department of Geology, Pleinlaan 2, 1050 Brussels, Belgium.*
† Electronic Supplementary Information (ESI) available

Introduction

The continuously improving sensitivity, precision and spatial resolution of modern analytical techniques, applied to a diversity of (extra-)terrestrial materials, constantly refine our view on the cosmochemical history of the early solar system and even lead to a deeper understanding of the processes taking place before its formation.[1,2]

Extraterrestrial materials are available from various sources, with meteorites being the most common, falling in great numbers on the surface of the Earth. Of these, iron meteorites are the most widespread, not only because of their resistance to weathering and a higher survival rate during atmospheric entry, but also because of the higher likelihood that these will be recognized as unusual objects. Iron meteorites fall into 14 major chemical groups[3], with chemical trends within most iron meteorite groups consistent with fractional crystallization, implying that each group formed from a single molten metallic pool or core. This is not the case for the silicate-bearing iron meteorite groups (IAB and IIE), with textures and poorly defined elemental trends that suggest that impact mixed molten metal and silicates and that neither group formed from a single isolated metallic melt.[3] The chemical classification of iron meteorites is based on the contents of and ratios between particular elements, mainly Ga, Ge, As, Ir, Ni and Au.

Bulk concentrations of several elements in iron meteorites are used to reveal the crystallization history of their parent bodies.[3] Except for the elements mentioned above, together with a few others, such as Pt, Os and Au, the pool of analytical data for particular elements in iron meteorites is rather small. Among the elements for which information is scarce, Ru, Rh, Pd and Pt are the most interesting. Nichiporuk and Brown[4] found that iron meteorites fall into 3 major groups with regard to their Ru-Rh concentrations and these groups correlate with the Ga-Ge groups found by previous researchers. More detailed data on fractionation of Rh in iron meteorites were presented by Ryan et al.[5] In both studies, Ru, Rh, Ir and Pt were found to correlate positively with each other. Hoashi et al.[6] show that the combination of concentration data for several platinum group elements (PGEs) can provide a more powerful tool for taxonomic classification of iron meteorites than the more common approach with Ir alone. At the same time, Pd concentrations span a range of about one order of magnitude and show negative correlation with Ru, Rh, Ir and Pt. Unlike the other PGEs, Pd correlates positively

with Ni.[5, 6] This exceptional fractionation behavior must result from the non-refractory nature of Pd.[7]

ICP-mass spectrometry (ICP-MS) is the most sensitive technique for (ultra)trace elemental analysis. While in its standard configuration, an ICP-MS instrument is intended for analysis of aqueous solutions, use of laser ablation (LA) as a means of sample introduction permits the direct analysis of solid samples as well. In addition, laser ablation – ICP – mass spectrometry (LA-ICP-MS) gives access to the spatial distribution of elements inside the iron meteorites studied. Spatially resolved chemical analysis of extraterrestrial materials can give invaluable data on presolar grains, dust and refractory inclusions.[8] Element diffusion profiles across the lamellae of iron meteorites provide information on the crystallization of molten metal and cooling rates of the meteorite parental bodies.[9] Together with Re, Mo and W, the PGEs (with exception of Pd) have condensation temperatures above that of Fe-Ni alloy, leading to the formation of refractory nuggets (fremdlinge) in chondritic material during nebula solidification.[7] Spatially resolved determination of Re and Os also improves the understanding of their fractionation mechanisms between mineral phases, applicable to building potential isochrones basing on Os isotope ratio measurements of individual phases.[10]. Although there is a lot of data available on the bulk concentrations of several elements in iron meteorites, their lateral distribution remains largely unstudied. It is mostly because EPMA and SEM-EDX, the most commonly applied methods for such spatially resolved analysis, do not show sufficiently low limits of detection (LoDs) for these elements. Moreover, the analytical techniques mentioned above are scarcely used for two-dimensional element imaging and are only applied for spot analysis or one-dimensional profiling. However, two-dimensional element imaging in combination with data correlation analysis is a promising tool to reveal the fractionation behavior of the elements inside the parent bodies of iron meteorites.

Next to elemental analysis, also isotopic analysis of meteorites is an attractive tool to shed light onto the history of the early Solar System and astrophysical processes. Variation in the isotopic composition of particular elements can serve as a sensitive tracer of stellar nucleosynthesis and as a tracer of heterogeneity of the solar nebula.[11, 12, 13] Isotopic analysis can yield chronological constrains on the formation of the first objects in the Solar System, when applied to several short- and long-lived isotopic decay systems in extraterrestrial material.[7, 14, 15, 16, 17] Although the capabilities of LA-ICP-MS for direct isotopic analysis are compromised by the co-presence of elements causing spectral interference, LA systems have been coupled to multi-collector-ICP-MS and used for high precision isotopic analysis of Mg, Si and Fe in meteorites.[18, 19] Importantly, LA-ICP-MS can provide fast and quasi-nondestructive analysis of iron meteorites for their elemental composition, an essential first stage for the subsequent investigation of isotopic systems of interest.

In view of the above, further assessment of the capabilities of LA-ICP-MS, a technique for high-resolution spatially resolved analysis with a potential of chemical and isotopic analysis, in this context will likely contribute to our understanding of the solar system formation. Previous works have focused on the comparison of the precision, accuracy and consistency of ns-LA-ICP-MS data for iron meteorites with data obtained via instrumental neutron activation analysis (INAA) and isotope dilution mass spectrometry (IDMS).[9, 20] In this work, we compare the LA-ICP-MS approach with other ICP-MS based techniques: pneumatic nebulization (PN) ICP-MS, discussed in detail by Folco et al.[21], and ID-PN-ICP-MS in combination with target element isolation using anion exchange chromatography. Special attention is paid to element mapping with LA-ICP-MS, widely used in geological applications to build element distribution maps.[22] Matrix effects, appearing due to interaction of the nanosecond laser pulse with iron phases showing different properties and their possible effect on the element distribution maps are also discussed.

Experimental

Reagents, certified reference materials (CRMs) and samples

Only high-purity reagents and acids were used throughout the experiments. Pro analysis grade nitric (65%, Chem-Lab, Belgium) and hydrochloric (37%, Chem-Lab, Belgium) acids were additionally purified by sub-boiling in a PFA and quartz apparatus, respectively. Water was purified (18.2 MΩ·cm) in a Direct-Q 3 water purification system (Millipore, France).

The 1000 $\mu g \cdot ml^{-1}$ single-element stock solutions used for external calibration originated from Merck (Darmstadt, Germany), PlasmaCAL (Quebec, Canada), Inorganic ventures (Virginia, USA) and Alfa Aesar GmbH (Karlsruhe, Germany). High purity Pt and Pd standards of natural isotopic composition, used for reverse ID-ICP-MS determination of the spike concentrations, were NBS 680 Pt (National Institute of Standards and Technology, Maryland, USA) and 99.9+%, Pd (Aldrich Chem Co) metals. Isotopically enriched Ru, Pd, Ir and Pt powdered metals were obtained from Oak Ridge National Laboratory (Tennessee, USA). Isotopic abundances are 97.70%, 98.86%, 99.59% and 91.46% for ^{101}Ru, ^{108}Pd, ^{193}Ir and ^{194}Pt, respectively.[23] The certified reference materials used in LA-ICP-MS analysis are listed in the ESI.

Seven iron meteorite specimens (4 from Russia, 1 from Kazakhstan, 1 from Australia and 1 from the USA) were obtained from different sources (see table 1). For two of these (Sikhote-Alin and Canyon-Diablo), the concentrations of several elements of interest have been published earlier, providing reference data for the validation of our results. The other meteorites have not been studied in detail via modern analytical methods.

Determination of the relative sensitivity factors in iron-matrix CRMs

Steel CRMs were polished with silicon carbide sandpaper (P4000 grit size, i.e. 2.5 µm median particle diameter). A New Wave Research UP193HE ArF* excimer-based LA-system (New Wave Research, CA, USA) coupled to a quadrupole-based XSeries II ICP-mass spectrometer (Thermo Fisher Scientific, Germany) was used to measure the signal intensities of the elements contained in the iron and glass CRMs selected (see ESI for instrument settings used). Pre-ablation was always applied to avoid possible contamination (400 µm beam diameter, 20 $\mu m \cdot s^{-1}$ lateral scanning speed, 5 $J \cdot cm^{-2}$ energy fluence). Relative sensitivity factors (RSFs) of the elements were calculated relative to Cu according

to the equation:

$$RSF_x = \frac{I_x \cdot C_{Cu}}{C_x \cdot I_{Cu}} \cdot \frac{A_{Cu}}{A_x}$$

where I_x, I_{Cu} are the intensities for the nuclide of interest and for ^{63}Cu, C_x and C_{Cu} are the concentrations of the element of interest and of Cu in the CRM and A_x and A_{Cu} are the relative isotopic abundances of the nuclide measured and of ^{63}Cu, respectively.

Bulk LA-ICP-MS

Thick sections of the iron meteorites were polished with silicon carbide sandpaper (grit size P4000) and lightly etched in a 4% v/v nital (HNO_3 in ethanol) solution to reveal the widmanstätten pattern. A New Wave Research UP-213 Nd:YAG LA-system coupled to a Thermo Scientific ELEMENT 2 sector field ICP-mass spectrometer was used for direct analysis of solid meteorites without digestion. Instrument settings of the ICP-MS and LA-units are summarized in table 2. Laser ablation was performed in line-scan mode with each line 1.8 mm long and 100 µm wide. A total of three lines were ablated on each sample and at least 5 lines on external standards. Pre-ablation was always applied to avoid the effect of possible surface contamination (150 µm beam diameter, 20 µm·s^{-1} translation speed, 5 J·cm^{-2} fluence).

The well-characterized Canyon Diablo IAB iron meteorite and NBS1286 low-alloy steel CRM from NIST were used for external calibration. The data set of concentrations determined for Canyon Diablo is compiled in the ESI. The compositional homogeneity and distribution of elements within this meteorite was discussed by Wasson et al.[24] ^{60}Ni was used as internal standard and previously reported Ni concentrations in the iron meteorites studied were relied upon.

LA-ICP-MS element mapping

A thick section of the IIC Darinskoe iron meteorite was chosen for elemental mapping because of a complex PGE distribution and relatively high content of the elements of interest. Just before the measurement, the surface was polished with silicon carbide sandpaper (grit size P4000) and etched with 4% v/v nital solution. A New Wave Research UP-213 Nd:YAG LA-system was coupled to a Thermo Scientific ELEMENT 2 sector field ICP-mass spectrometer for elemental mapping, using the instrument settings summarized in table 2.

The Cheder IID iron meteorite was used as external standard for LA-ICP-MS mapping, because of its fairly high content of PGEs, similar to that in Darinskoe. The concentration values used for calibration were taken from Agafonov et al.[25] In total, 72 straight lines were ablated one next to the other without space in-between to form a rectangular surface area of 2800 x 2880 µm. ICP-MS signal monitoring was triggered by the LA-system and the results thus obtained were used to construct intensity and concentration maps.

Pneumatic nebulization ICP-MS

The protocol was based on that described in Folco et al.[21] Iron meteorite fragments were cut off the bulk mass with a diamond disk saw. To avoid the effect of surface contamination, visibly altered (*i.e.* oxidized) surfaces were cleaned with silicon carbide sandpaper, subsequently etched in dilute HNO_3 in an ultrasonic bath and finally rinsed with ethanol. Fragments of about 100 mg were accurately weighed and transferred into 15 ml Savillex™ Teflon beakers and digested in 4 ml of freshly prepared aqua regia (HNO_3:HCl 1:3). For that purpose, the closed vessels were heated at 90˚C during 72 hours. The resulting digests were diluted to 50 ml with Milli-Q water, followed by an additional 500-fold dilution for Cr, Co, Ni and Cu and a 4-fold dilution for all of the other elements in 0.4 M HCl – 0.2 M HNO_3. The final solutions were introduced into a Thermo Scientific ELEMENT 2 sector field ICP-mass spectrometer via nebulization. Instrument settings are summarized in table2. Medium mass resolution (M/ΔM=4000) was used to resolve potential spectral interferences. Arsenic (As) was measured interference-free in high mass-resolution mode (M/ΔM=10000). Quantification was performed relying on external calibration, using synthetic mixtures of single-element stock solutions diluted to concentration levels similar to those in the samples. To correct for matrix effects, instrument drift and signal instability V, Rb and Bi were used as internal standards.

ID-PN-ICP-MS determination of PGEs

Isotopically enriched Pd and Pt metal standards of approximately 5 mg were accurately weighed and dissolved in 4 ml of freshly prepared aqua regia in 15 ml Savillex™ Teflon beakers, heated at 140˚C for 72 hours. After cooling down, the beakers were opened and the solutions were evaporated to incipient dryness and the residue redissolved in 0.4 ml of concentrated HCl. This was repeated twice. Finally, the residues were re-dissolved in 10 ml of 50% HCl. The Ru and Ir metal spikes were fused with Na_2O_2/NaOH in Al_2O_3 crucibles using a Bunsen torch and the resulting melts were dissolved in 30% HCl.

Iron meteorite fragments were cut off a bulk mass and cleaned in the same way as those prepared for PN-ICP-MS. The chips were accurately weighed into 15 ml Savillex™ Teflon beakers and appropriate amounts (0.1-0.5 ml) of dilute Ru, Pd, Ir and Pt spike solutions were added gravimetrically. This was followed by digestion with 4 ml of aqua regia at 140 °C for 48 hours. The solutions were evaporated to near-dryness, re-dissolved in 2 ml of concentrated HCl and evaporated to dryness again. This procedure was repeated twice. Finally, all sample residues were re-dissolved in 10 ml of 0.5 M HCl. Air buoyancy corrections, negligible for standard ICP-MS measurements, were applied for all weighing and dilution steps prior to ID-PN-ICP-MS.

Column anion-exchange isolation of PGEs, Au and Re

10 ml polypropylene columns (Eichrom) were packed with 1.5 ml of Eichrom AG 1X-8 anion exchange resin (mesh size 100-200). The resin was washed with 10 ml of Milli-Q water, 10 ml of 4 M HNO_3 and 10 ml of 6 M HCl and subsequently equilibrated with 10 ml of 0.5 M HCl. All 10 ml of sample solution was loaded onto the column and the matrix was eluted off with 10 ml of 0.5 M HCl and 10 ml of 0.8 M HNO_3. Subsequently, the PGEs, Re and Au were collected using 50 ml of hot (90 ˚C) concentrated HNO_3. Solutions were evaporated to dryness, 0.4 ml of fresh aqua regia was added and the closed vessels were heated at 140˚C for 24 hours and subsequently opened and the digest evaporated to dryness. This procedure was repeated twice to destroy organic material originating from anion-exchange resin decomposition. Finally, the residues were dissolved in 0.6 M HNO_3 – 0.1 M HCl

prior to the measurement.

Isotope ratio measurement for ID-PN-ICP-MS

Ru, Pd, Ir and Pt isotope ratios were measured using a Thermo Scientific ELEMENT XR ICP-mass spectrometer in the standards with a natural isotopic composition, the isotopic spike solutions and meteorite material equilibrated with the PGE isotopic spikes after chromatographic isolation. The instrument settings used for this purpose are summarized in table 3.

For isotope dilution analysis, the Element XR ICP-MS unit was optimized for fast mass-scanning and high precision of intensity ratios. The shorter the time gap between two isotopes measured, the higher the precision of the resulting ratio. Separate methods for all 4 elements were created to avoid the use of B-scanning and reduce the time gap mentioned above. Narrow mass windows and settling times were used. Low resolution was preferred because of the flat-topped appearance of the peaks and the corresponding higher isotope ratio precision.[26] The measurement time was 1 min 22 s for each element. The counting detection mode is preferable in this context, because it does not introduce a detector cross-calibration error to the ratios, but in this case care must be taken to fit the intensity into the maximum range. Therefore, the triple detection mode was chosen to protect the detector, but all the concentrations were adjusted to be in the range of counting detection mode (< $3 \cdot 10^6$ counts·s^{-1}). Isotope abundance ratios ^{99}Ru/^{101}Ru, ^{105}Pd/^{108}Pd, ^{191}Ir/^{193}Ir and ^{194}Pt/^{195}Pt were used in the calculations. The concentrations of Ru, Pd, Ir and Pt in the meteorites were calculated according to the equation[27]:

$$C_s = C_{tr} \cdot \frac{m_{tr}}{m_s} \cdot \frac{(R_{tr} - R_{bl})}{(R_{bl} - R_s)} \cdot \frac{f_{tr}}{f_s},$$

where C_s is the concentration of the element in the sample. C_{tr} is the concentration of the isotopically enriched solution, accurately determined by reverse ID-MS. These reverse ID-MS experiments relied on the use of PGE standard solutions prepared gravimetrically from high-purity metals. m_{tr} and m_s are the masses of the isotopically enriched solution and sample solution, respectively. R_{tr}, R_{bl} and R_s are the isotope ratios measured in the isotopically enriched spike solution, the sample-spike mixture and a standard with natural isotopic composition, respectively. f_{tr} and f_s are the isotopic abundances of the enriched isotope in the spike and in nature, respectively. f_{tr} values were taken from Vanhaecke et al.[23], where the same enriched materials were used. Extraterrestrial Ru, Pd, Ir and Pt were assumed to show a natural isotopic composition [28] and diluted standard solutions of natural isotopic composition were used instead of non-spiked sample to save precious meteorite material. Mass bias correction was not applied as all ratios are measured under identical experimental conditions and thus, instrumental mass discrimination is automatically corrected for.[29]

Results and discussion

ns-LA-ICP-MS matrix effects

Next to sample heterogeneity, spectral interferences, lack of proper reference materials, also matrix effects are known to affect the quantitative results obtained via ns-LA-ICP-MS. The differences in physical properties of materials lead to different characteristics of laser-solid interaction and aerosol formation.[30, 31] As a result, material transport from the solid sample to the detector of the mass spectrometer can be non-stoichiometric, resulting in a change of the relative sensitivity factors (RSFs) from one type of matrix to another.[32]

A first conclusion based on the RSFs obtained (figure 1) is that the widely used glass CRMs are not suited as external standards in the analysis of iron materials. The absolute sensitivity observed for glass materials is almost two orders of magnitude higher than that for a metal matrix and, even more important, the RSFs determined for glass CRMs are significantly different from those for CRMs with an iron matrix (figure 1 B). This means that matrix-matched calibration is a prerequisite.

Four certified reference materials with different iron matrices were analyzed using identical instrument settings; the corresponding results are shown in figure 1. Even among iron materials, substantial differences in ablation efficiency were observed: the differences in the absolute sensitivities (figure 1 A) are significantly larger than the associated analytical uncertainty. At the same time, normalization of absolute sensitivities to the sensitivity of an element with known concentration provides RSFs for different iron CRMs, which are identical within statistical error (figure 1 B). This implies that internal normalization is crucial in the case of analysis of iron materials with ns-LA-ICP-MS.

In the same manner, the different metal phases within an iron meteorite, distributed heterogeneously inside most meteorite fragments, also have different ablation efficiencies. Figure 2 shows the intensity distribution map in the thin section of the Darinskoe IIC iron meteorite. Fe and Ni are seemingly enriched in the same spots of the intensity map. As these two elements compose the matrix of the meteorite, the combined increase of both Fe and Ni can only be explained by a change of the ablation efficiency from one metal phase to another and this effect should be corrected for by internal standard normalization.

Quantification of ns-LA-ICP-MS data

For bulk LA-ICP-MS analysis, sufficiently large total areas are ablated, the Ni intensities were averaged and used as internal standard and Ni concentration values were taken from literature. This internal standardization procedure was found sufficiently accurate and was relied upon for bulk LA-ICP-MS analysis. Alternately, one can also deploy an independent analytical method (e.g., EPMA, SEM-EDX, XRF) to determine the concentration of one of the matrix elements (Co or Ni) and apply this as internal standard.[9, 20] The principal challenge of internal standardization for the element mapping is that none of the iron meteorites contains a homogeneously distributed element that could serve as an internal standard. Therefore, for spatially resolved LA-ICP-MS analysis, the following well-known approach [33, 34, 35] was used: Fe and Ni were considered to contribute 100% of the matrix and thus, the sum of their intensities was used as a virtual, evenly distributed internal standard.

Unfortunately, there are no CRMs of matrix-matched composition with the elements of interest certified at a concentration level close to that of iron meteorites. Previous studies[36] have used doped NiS beads as external standards for

quantification in iron meteorite analysis, relying on the fact that NiS and FeNi matrices should have similar physical properties. Elements like Co, Ni, Mo and W can be quantified straightforwardly by application of different steel CRMs, but the only approach to quantify PGEs, Ga, Ge, etc. is to use an iron meteorite with well-known analyte concentrations. The meteorite used as external standard is required to have significant concentrations of the elements of interest, which need to be homogeneously distributed and, even more importantly, the concentrations of these analytes need to be well-known. As such an external standard does not have certified values, an accurate survey of literature data becomes necessary. Campbell et al.[9, 33, 34, 37] and Petaev et al.[20] applied IVB Hoba and IIA Filomena iron meteorites and a set of NIST steel CRMs (1158, 1263) as external standards. Hoba has a relatively high content of PGEs (4.86-42.48 µg/g), while Filomena is a hexahedrite with a homogeneous element distribution. In the present work, we have selected the IAB Canyon-Diablo iron meteorite as an external standard as it is one of the best-studied iron meteorites and is widely available.

LA-ICP-MS element mapping

The maps presenting the distribution of elements over the thick section of Darinskoe IIC iron meteorite are shown in figure 3. Trends of the Fe and Ni concentrations coincide with the Widmanstätten pattern, visible in the reflected light image. Based on the spatially resolved quantitative data generated for the Darinskoe IIC iron meteorite, a matrix of Pearson's product-moment correlation coefficients was calculated (table 4). This correlation matrix provides information on the general trends that exist between the elements within space-distributed data. The closer the element-element correlation coefficient is to ±1, the higher the linear correlation between the pair of elements considered, while a value of 0 means absence of correlation. The calculated coefficients are not very high, only coefficients for Os, Ir and Pt are higher than 0.8. We treated the coefficients higher than 0.4 or lower than -0.4 as positive or negative correlation, respectively. For example, Ni-Fe show strict negative correlation as a result of our normalization procedure, that uses a "Fe+Ni = 100%" approach.

Ni correlates negatively with Co and Ge, indicating that Co and Ge became concentrated in Fe-rich kamacite lamellas during the cool-down of the Darinskoe IIC meteorite body. Interestingly, W, another refractory element, doesn't correlate neither with Ni nor with Fe and seems to correlate positively only with the heavy PGEs (HPGEs: Ir, Os and Pt).

Five of the six PGEs (Ru, Rh, Os, Ir, Pt) show a positive correlation with each other. Among them, the HPGEs seem to show a stronger correlation to each other than to the light PGEs (LPGEs: Ru, Rh, Pd). This indicates that PGEs have the same trend of fractionation during cool-down of the meteorite parent body, while the degree of fractionation is slightly different for light and heavy PGEs. Also, analysis shows that PGEs are not found to concentrate in kamacite or taenite lamellas, but correlate positively with Ga and Ge. Interestingly, one of the LPGEs – Pd – does not show any correlation with any of the elements. It can be a demonstration of its different fractionation behavior, but it can also be caused by the fact that the levels of Pd are closer to its LoD than for the other PGEs and hence, the Pd data suffer more from noise.

Two refractory elements – the lithophile W and the siderophile Au – both show only a weak positive correlation (0.42-0.47) to HPGEs, which means that they tend to concentrate together with them spatially inside the meteorite.

Re is dispersed over the meteorite matrix and does not correlate with any other element. An inclusion of about 50 µm that is enriched in Re (5-10 µg/g) and PGEs can clearly be recognized in the middle right of the image. Such Re-containing nuggets can strongly influence the $^{187}Os/^{188}Os$ ratio, as ^{187}Os is produced by radioactive decay of ^{187}Re. Thus, the Re-Os chronometry results can discord with those based on the Pt-Os system (involving $^{186}Os/^{188}Os$ isotope ratio determination) as – in contrast to Re – Pt and Os are fairly homogeneously distributed.

Comparison of the concentration range in the element maps for Darinskoe IIC (figure 3) with the ranges characteristic for the IIC group meteorites demonstrate agreement (see figure 4). The only significant exception is Ru, the range of which seems to be too high for IIC group.[6] Possibly, the Ru result can show bias because the reference value for the external standard Cheder IID is not very well characterized.

Comparison of mapping LA-ICP-MS with micro-XRF

Mapping of the Darinskoe meteorite section was also done with a home-built micro-XRF spectrometer over an area of 2700 x 2775 μm^2 by measuring 37 x 112 points. Each point was measured for 50 s with an estimated photon flux of $1.2 \cdot 10^7$ photons per second, applying 0.400 mA and 40 kV tube settings. The micro-XRF setup was based on a XOS DCC-X-Beam Mo anode source coupled with doubly curved crystal (DCC) optics providing a 150 x 50 μm^2 monochromatic x-ray beam (compare with 40 µm beam diameter in LA-ICP-MS). Quantitative elemental information was obtained from the acquired XRF spectra through Monte Carlo simulations by the iterative process of simulating the experiment.[38, 39] Reference experimental parameters needed for modeling were acquired by measuring well known CRMs with different matrices. The comparison of the results from both methodologies may validate the LA-ICP-MS quantification procedure.

As the map was obtained for a physically different position than the LA-ICP-MS map, it was not possible to compare them directly. Nevertheless, figure 5 presents the comparison of the Ni and Fe/Ni distribution of all the individual pixels. The average concentration for Fe and Ni is 83.9 % and 11.0 % respectively according to XRF. Note that the width of the distributions is substantially wider in the case of LA-ICP-MS, which can be attributed to the higher spatial resolution of the LA-ICP-MS approach and/or to the noisier signal with LA-ICP-MS. Given the relatively small difference in terms of spatial resolution of the methods (slightly better for LA-ICP-MS in this example), the latter explanation is more probable. Indeed, for each point the signal is acquired during 50 s for the micro-XRF mapping, while the corresponding time in LA-ICP-MS is only 4s. In the case of micro-XRF, a longer acquisition time is possible owing to non-destructive nature of the technique. The total acquisition time for mapping of the selected area LA-ICP-MS was approximately 5 hours, while for micro-XRF the corresponding time was 57 hours.

The LoDs for micro-XRF and for LA-ICP-MS in mapping mode are almost comparable. The LoDs for LA-ICP-MS in

mapping mode are 0.5-20 µg/g for PGEs and other micro-elements. This level is 2-5 times higher than LoDs obtained for bulk LA-ICP-MS. In case of micro-XRF, the LoDs are in the range of 20-40 µg/g for Ga and Ge for the individual spectra of the acquired XRF map, while the LoDs of PGEs were not good enough for their determination.

PGE separation and ID-PN-ICP-MS

Low concentrations of PGEs ($1 \cdot 10^{-3}$-10^{2} µg/g) in iron meteorites and the necessity of high dilution due to the heavy iron matrix are decreasing the concentrations at which the target elements occur in the solutions to be measured and to values close to the LoDs and challenge their determination by ICP-MS. Moreover, Fe, Ni and Cu, composing the matrix of iron meteorites, form argide species in the plasma which can severely interfere with some target elements. This stresses the merits of separating and pre-concentrating PGEs prior to ICP-MS measurement. Fortuitously, the PGEs, Re and Au show high affinity to anion exchange resins in a dilute HCl medium.[40] At the same time, this separation approach faces problems of low recoveries due to difficulties of complete elution[41, 42, 43] and strong retention dependence on the sample pretreatment.[41, 44, 45]Due to difficulties in reaching quantitative recoveries, the isotope dilution approach became widespread. When isotope ratios are measured instead of absolute intensities, this method is not sensitive for analyte losses, provided these occur after isotope equilibration is reached.

The anion exchange column separation of Ru, Rh, Pd, Ir, Pt, Au and Re from the iron matrix using Dowex AG 1X-8 anion exchange resin (100-200 mesh) in 0.5 M HCl medium is based on procedures described in Hann et al.[27], Hodge et al.[46], Colodner et al.[47] and Müller et al.[48] Isolation of volatile Os, which escapes during the digestion as tetroxide, is not possible without additional measures[45] and was beyond the scope of this work. Elimination of Fe, Ni, Co, Zn, Cu, Mo and Cd was of interest in the context of PGE determination in iron meteorites. Siderophile Co, Ni, Cu and, to some extent, chalcophile Zn, are abundant in iron meteorites and can form argide ions that overlap with the signals of the light PGEs in ICP-MS analysis. Molybdenum, present in concentrations close to those of the PGEs, results in isobaric overlaps with Ru and forms oxides that interfere with the determination of Pd. Cadmium, although being very rare in meteorites, has isobars with Pd. The importance of Zr and Hf separation is widely discussed by Pearson et al.[45] but these lithophile elements have extremely low concentrations in iron meteorites and thus, are irrelevant in the context of this work.

The experimental elution curves, built relying on data obtained for a synthetic mixture of elements, are shown in figure 6 and the numeric figures of merit for the separation are listed in the ESI. 0.5 M HCl was used to wash off all the Fe, Co, Ni and Cu. Subsequently, 0.8 M HNO_3 was used to elute all possible Cd and Zn. A minor tail of Mo can be observed in the analyte fraction. Hot concentrated nitric acid was then used to elute the analytes from the resin. Elevated levels of ubiquitous Fe and Zn originate from the lab environment and likely from the resin decomposed by HNO_3. These amounts of Fe, Zn and Mo after the separation correspond to 0.1, 0.05 and 0.03 µg respectively, corresponding to separation coefficients of about 10^{3}-10^{4} in the case of real meteoritic element abundances. The anion exchange resin can be used only once, because it is partially digested by the hot nitric acid. Blanks of the chromatography are negligible compared to the levels of analytes processed.

As soon as isotopic equilibration is achieved during the digestion, losses of the elements of interest will not affect the results of ID-ICP-MS analysis (the recoveries are 43-70% for Ru, Pd, Ir, Pt). The mono-isotopic element Rh cannot be determined by isotope dilution and non-quantitative recovery prevents its determination by external calibration. Rhenium and the mono-isotopic Au show relatively high recoveries in this separation and can be determined by PN-ICP-MS without isotope dilution. The performance of anion exchange column chromatography and ID-PN-ICP-MS measurements were verified by analyzing Canyon Diablo meteorite for which the concentrations of the elements of interest are well-documented. The results were found to be in a good agreement with the reference data, which proves the suitability of the method for the purpose of iron meteorite analysis. The concentrations of Ru, Pd, Ir, Pt, Au and Re in 4 iron meteorites, determined by the approach described above are shown in table 5**.** The results demonstrate very good agreement with the reference data, available in literature (figure 7, C).

Comparison of bulk LA, pneumatic nebulization and ID-PN-ICP-MS analysis

The intensities for ^{74}Ge, ^{75}As, ^{103}Rh and ^{105}Pd were corrected for the contribution from NiO^{+}, $NiOH^{+}$ and $ArCu^{+}$ interferences. For this correction, their extents of formation were determined by analyzing NBS 1286 steel CRM that contains no Ge, As or PGMs. No significant differences were found between interference-corrected and non-corrected results in laser ablation mode.

The LoDs for bulk LA-ICP-MS, pneumatic nebulization ICP-MS and for anion exchange ID-PN-ICP-MS analysis of iron meteorites are shown in table 5. LoDs for LA-ICP-MS are based on 3s of the gas blank and the sensitivity, calculated using the Canyon Diablo iron meteorite. The LoDs for solution nebulization are calculated as 3s of the acid blanks, which went through all the stages of decomposition, similar to the samples. For ID-PN-ICP-MS, LoDs were calculated using a formula, developed by Yu et al.[49] According to the formula, LoDs are calculated as a function of the enrichment of the isotopic spike and the external calibration LoDs. Taking the dilution into account, the LoDs with PN-ICP-MS are 1-2 orders of magnitude lower than those for LA-ICP-MS at the spot size used. The elevated LoDs for Co, Cu, Ni, Mo and Pd in LA-ICP-MS mode can be explained by memory effects in the instrumentation applied. The LoDs for anion exchange ID-PN-ICP-MS are 1-2 orders of magnitude lower then ones for PN-ICP-MS, because high dilution is not needed since the matrix is removed chromatographically.

It is important to stress that in LA-ICP-MS, LoDs depend on the experimental conditions: laser frequency, beam diameter and energy fluence. The LoDs presented here are calculated for the experimental parameters shown in table 2. The LoDs for LA-ICP-MS reported here, are almost similar to those for the point analysis mode LA-ICP-MS, reported by Campbell and Humayun.[9] These authors used a similar sector field based Element ICP-MS unit and a 266 nm Nd:YAG solid state LA-system. For a similar experimental approach with line-scanning, Campbell and Humayun[9] presented 100-fold lower LoDs at levels

not achievable in our study. Several ways to improve the LA-ICP-MS LoDs can be applied. Application of He as a cell-gas is a well-known method to increase the sensitivity of LA-ICP-MS with about one order of magnitude. Unfortunately, He was not available in our experimental setup. Admixture of N_2 into the ICP is also a widely-used strategy to enhance the sensitivity[50], found to give a 5-fold improvement, but at the same time, this leads to significant increase of the level of interferences at the masses of Mo, Ge and As and this approach was therefore not used.

The LoDs, achieved in this work for PN-ICP-MS at medium mass resolution are comparable to those for quadrupole-based ICP-MS after similar digestion and dilution procedures (see Folco et al.[21]). The LoD for As is much higher than those of other elements because of the application of the high resolution mode.

The relative standard deviation (RSD) on the LA-ICP-MS signals (below 15% in the most cases) is on average two times higher than that using PN-ICP-MS. The distributions of all the RSDs obtained in this work are shown in figure 8. It is important to note that many of the elements are only contained in the meteorites studied in amounts close to their LA-ICP-MS LoDs. The standard deviation for the laser ablation mode appears to depend on the proximity to the LoD: it increases severely at lower concentration levels. Dependence of the RSD on the concentration level is shown in figure 9. The RSD in PN-ICP-MS is within 1 to 7% for most analytes, which is comparable with the reported range (1-6%) for quadrupole-based ICP-MS after similar digestion and dilution procedures.[21] For ID-PN-ICP-MS, the RSD is below 5% in the most cases.

The results of LA-ICP-MS and PN-ICP-MS analysis of the iron meteorites are in fair to very good agreement. The concentrations of the PGEs, Au and Re, determined by different methods are plotted versus one another in figure 7 for comparison.

It is important to note some deviating values among the LA-ICP-MS results, which might appear due to non-homogeneous element distribution on the surface of the sampled thick section or insufficient representativeness of the area sampled. These effects of non-representativeness, being grain size-dependent, are difficult to control, because they can be less or more pronounced for different types of meteorites. As an example of the inhomogeneity effects, for the Darinskoe IIC iron meteorite, all values are discordant in bulk LA-ICP-MS (0.54 mm^2 total ablated area), but the average data from the mapping experiment with a sampled surface of 7.84 mm^2 coincide very well with the PN-ICP-MS data. For the same reason, some data were replaced by those obtained using an UP193HE ArF* LA-unit coupled to XSeries II ICP-MS instrument, because this setup allows to use a 400 µm beam size (1.52 mm^2 of total ablated area).

The composition of the 5 iron meteorites investigated demonstrates good agreement with the literature data for other iron meteorites of the same type on PGE-Ni diagrams (figure 4). Literature data are taken from Pernicka and Wasson[50], Hoashi et al.[6], Ryan et al.[5], Mermelengas et al.[51], Wasson et al.[52, 53, 54] and Rasmussen et al.[55] Chinga, which is known to be an anomalous representative of IVB, shows discordant behavior. Abundances of Ir and Pt correlate nicely with other meteorites of their groups. Not only for Ir and Pd, commonly used for classification, but also for the less studied PGEs Ru, Rh and Pd, the data fit well on the PGE-Ni diagrams. The only exception is the abundance of Ru in Cheder, which seems to be too high for IID. On the other hand, the 28 µg/g Ru concentration in Cheder, reported by Agafonov et al.[25] is also much higher than the range of Ru known for IID (Pernicka and Wasson[50], Hoashi et al.[6]). Meteorites of group IIC are very rare (only 8 known members) and to the best of our knowledge, we are the first to present abundances of PGEs and other elements in Darinskoe, which fit well with previously reported data for other IIC meteorites. The concentrations of Ru, Pd and Pt are slightly higher than their known range in the IIC group.

Conclusions

LA-ICP-MS is a sensitive method that allows obtaining bulk and spatially resolved element information for iron meteorites. It is especially suitable for fast and quasi-nondestructive analysis of precious extraterrestrial material. LA-ICP-MS has shown to be a valuable technique for iron meteorites, not only for homogeneous ataxites and hexahedrites, but also for more heterogeneous ones, when considering large enough total ablated areas.

We demonstrate a significant effect of the matrix on the interaction of the nanosecond laser pulse with various phases of the metal matrix. A quantification procedure with application of a matrix-matched external standard and proper internal standardization is required to correct for these, sometimes severe, matrix effects. Careless use of intensity distribution maps without proper correction for these matrix effects can lead to incorrect interpretations.

The LoDs for bulk LA-ICP-MS determination of trace elements in iron meteorites are in the range of 0.1-15 µg/g, which is higher than those reported in earlier works[9], but still sufficiently low for the determination of the elements of interest in almost all of the meteorites studied. The LoDs of PN-ICP-MS are 1-2 orders of magnitude lower than those of LA-ICP-MS and similar to values reported in literature. One possible way to improve the LoDs of the LA-ICP-MS analysis is to apply He as a cell gas, which was not possible in this work, because we did not have it our experimental setup. The LoDs with anion exchange ID-PN-ICP-MS ($3\cdot10^{-4}$-$2\cdot10^{-3}$ µg/g) are 1-2 orders of magnitude lower than those for PN-ICP-MS, because high dilution is not needed since the matrix is removed chromatographically. The RSD accompanying the results of LA-ICP-MS analysis of iron meteorites is below 15% in most cases, but increases when the concentration approaches the LoD. This high uncertainty can be explained by inhomogeneity in the element distribution on the surface. The RSD of PN-ICP-MS is 2-3 times lower than that typical for LA-ICP-MS (1 to 7%). For ID-PN-ICP-MS, the RSD is below 5% in the most cases.

Meteorites of IIC group are very rare (only 8 known members) and before this study, Darinskoe was the least studied member of the group. We present reliable abundances of PGEs and other elements in Darinskoe, which fit well with previously reported data for other IIC meteorites. Also, solid data are added for several meteorites that were poorly studied so far.

We have also provided information on the distribution of the analyte elements within the Darinskoe meteorite and demonstrated the application of correlation analysis in element imaging. In the context of elemental mapping using LA-ICP-MS,

correlation analysis is a powerful tool that can provide valuable information on the fractionation of the elements in the parent bodies of meteorites.

The most significant improvement in LA-ICP-MS analysis of iron meteorites is expected to result from the use of femtosecond LA-systems.[32, 35] In contrast to nanosecond LA, the duration of the femtosecond laser pulse is much shorter than the thermal and mechanical relaxation times in metal matrixes, which shifts the ablation processes to non-thermal mechanisms.[30] It results in higher aerosol formation efficiency, higher signal/background ratio, less element fractionation, less matrix effects and more stable signals. Application of sensitive fs-LA-ICP-MS systems in the future will also allow reducing the beam diameter without compromising the LoDs, which will enable precise elemental and isotopic data to be achieved for smaller inclusions.

References

1. G. J. MacPherson and M. H. Thiemens, *PNAS*, 2011, **108**, 19130-19134.
2. E. K. Zinner, F. Moynier and R. M. Stroud, *PNAS*, 2011, **108,** 19135-19141.
3. J. I. Goldstein, E. R. D. Scott and N. L.Chabot, *Chemie der Erde*, 2009, **69**, 293-325.
4. W. Nichiporuk and H. Brown, *Journal of geophysical research*, 1965, **70**, 459-470.
5. D. E. Ryan, J. Holzbecher and R. R. Brooks, *Chemical Geology*, 1990, **85**, 295-303.
6. M. Hoashi, R. R. Brooks and R. D. Reeves. *Chemical Geology*, 1993, **106**, 207-218.
7. H. Palme, *Elements*, 2008, **4**, 233-238.
8. A. M. Davis, *PNAS*, 2011, **108**, 19142-19149.
9. A. J. Campbell and M. Humayun, *Anal. Chem.*, 1999, **71**, 939-946.
10. T. Hirata and R. W. Neshbitt, *Earth and Planetary Science Letters*, 1997, **147**, 11-24.
11. E. Zinner, *Science*, 2003, **300**, 265-267.
12. G. J. MacPherson and A. Boss, *PNAS*, 2011, **108**, 19152-19158.
13. Q. Yin, S. B. Jacobsen and K. Yamashita, *Nature*, 2002, **415**, 881-883.
14. D.-C. Lee and A. N. Halliday, *Nature*, 1995, **387**, 771-774.
15. M. I. Smoliar, R. J. Walker and J. W. Morgan, *Science*, 1996, **271**, 1099-1102.
16. S. J. Woodland, M. Rehkämper, A. N. Halliday, D.-C. Lee, B. Hattendorf and D. Günther, *Geochimica et Cosmochimica Acta*, 2005, **69**, 2153-2163.
17. Y. Amelin and T. R. Ireland, *Elements*, 2013, **9**, 39-44.
18. E. D. Young, J. I. Simon, A. Galy, S. S. Russell, E. Tonui and Oscar Lovera, *Science*, 2005, **308**, 223-227.
19. I. Horn, F. von Blanckenburg, R. Schoenberg, G. Steinhoefel and G Markl, *Geochimica et Cosmochimica Acta*, 2006, **70**, 3677-3688.
20. M. I. Petaev and S. B.Jacobsen, *Meteoritics & Planetary Science*, 2004, **39**, 1685-1697.
21. M. D'Orazio and L. Folco, *Geostandards Newsletter*, 2003, **27**, 215-225.
22. T. Ulrich, S. S. Balz, K., Pedro, J. Jugo and D. K. Tinkham, *The Canadian Mineralogist*, 2009, **47**, 1001-1012.
23. S. Compernolle, D. Wambeke, I. De Raedt and F. Vanhaecke, *Spectrochimica Acta B*, 2012, **67**, 50-56.
24. J. T. Wasson and X. Ouyang, *Geochimica et Cosmochimica Acta*, 1990, 54, 3175-3138.
25. L. V. Agafonov, V. A. Popov, G. N. Anoshin, L. N. Pospelova, V. I. Zabelin and V. I. Kudryavtsev, *Russian Geology and Geophysics*, 2011, **52**, 620-630.
26. F. Vanhaecke, Luc Moens and Richard Dams *Anal. Chem.*, 1996, **68**, 567-569.
27. S. Hann, G. Koellensperger, K. Kanitsara and G. Stingedera, *J. Anal. At. Spectrom.*, 2001, **16**, 1057-1063.

Acknowledgments

This research has been funded by the Interuniversity Attraction Poles Program initiated by the Belgian Science Policy Office. Steven Goderis is a postdoctoral fellow of the Research Foundation – Flanders (FWO).

The collection of iron meteorites from east Russia and northern Kazakhstan was kindly donated by dr. F.P. Lesnov (IGM SB RAS). Miles and Canyon Diablo were provided by the Royal Belgian Institute of Natural Sciences.

The authors appreciate the generous help of Barbara Van Langenhove (OCAS NV) with LA-ICP-MS measurements at OCAS laboratory and kindly acknowledge Maarten Moens (Umicore Precious Metals Refining) for Na_2O_2/NaOH fusion of Ru and Ir metal spikes.

28. R. W. Carlson, S. B. Shirey and M. Schönbächler, *Elements*, 2008, **4**, 239-245.
29. K. G. Heumann, S. M. Gallus, G. Rädlinger and J. Vogl, *J. Anal. At. Spectrom.*, 1998, **13**, 1001-1008.
30. D. Bleiner and A. Bogaerts, Spectrochimica Acta Part B, 2006, Vol. 61, P. 421-432.
31. M. Holá, V. Konečná, P. Mikuška, J. Kaiser and Viktor Kanický, *Spectrochimica Acta Part B*, 2010, **65**, 51-60.
32. V. Možná, J. Pisonero, M. Holá, V. Kanický and D.Günther, *J. Anal. At. Spectrom.*, 2006, **21**, 1194-1201.
33. A. J. Campbell, M. Humayun and M.K. Weisberg, *Geochimica et Cosmochimica Acta*, 2002, **66**, 647-660.
34. A. J. Campbell, M. Humayun, A. Meibom, A. N. Krot and K. Keil, *Geochimica et Cosmochimica Acta*, 2001, **65**, 163-180.
35. H. Wiltsche and D. Günther, *Anal. Bioanal. Chem.*, 2011, **399**, 2167-2174.
36. E. Mullane, O. Alard, M. Gounelle and S. S. Russell, *Chemical Geology*, 2004, **208**, 5-28.
37. A. J. Campbell and M. Humayun, *30th Annual Lunar and Planetary Science Conference*, 1999, Houston, TX, abstract 1974.
38. T. Schoonjans, L. Vincze, V. A. Sole, M. S. Del Rio, P. Brondeel, G. Silversmit, K. Appel and C. Ferrero *Spectrochimica Acta Part B*, 2012, **70**, 10-23.
39. T. Schoonjans, V. A. Sol, L. Vincze, M. S. D. Rio, K. Appel and C. Ferrero, *Spectrochimica Acta Part B*, 2013, **82**, 36-41.
40. I. Matsubara, Y. Takeda, K. Ishida, *Fresenius J. Anal. Chem.*, 2000, **366**, 213-217.
41. I. Jarvis, M. M. Totland and K. E. Jarvis, *Analyst*, 1997, **122**, 19-26.
42. T. Meisel, J. Moser, N. Fellner, W. Wescheider and R. Schoenberg, *Analyst*, 2001, **126**, 322-328.
43. P. Kovacheva and R. Djingova, *Analytica Chimica Acta*, 2002, **464**, 7-13.
44. Y. V. Yi and A. Masuda, *Anal. Chem.*, 1996, **68**, 1444-1450.
45. D. G. Pearson and S. J. Woodland, *Chemical Geology*, 2000, **165**, 87-107.
46. V. Hodge, M. Stallard, M. Koide and E. D. Goldberg *Anal. Chem.*, 1986, **58**, 616-620.
47. D. C. Colodner, E. A. Boyle and J. M. Edmond, *Anal. Chem.*, 1993, **65**, 1419-1425.
48. M. Müller and K. G. Heumann, *Fresenius J. Anal. Chem.*, 2000, **368**, 109-115.
49. L. L. Yu, J. D. Fassett and W. F. Guthrie, *Anal. Chem.*, 2002, **74**, 3887-3891.
50. E. Pernicka and J. T. Wasson, *Geochimica et. Cosmochimlca Acta*, 1987, **51**. 1717-1726.
51. N. Mermelengas, R. De Laeter and K. J. R. Rosman, *Geochim. Cosmochim Acta*, 1979, **43**, 747-753.
52. J. T. Wasson, H. Huber and D. J. Malvin, *Geochimica et Cosmochimica Acta*, 2007, **71**, 760-781.
53. J. T. Wasson, *Geochhica et Cosmochimica Acta*, 1960, **33**, 860-876.
54. J. T Wasson and Wang Jianmin, *Geochimica et Cosmochimica Acta*, 1986, **50**, 725-732.

55. K. L. Rasmussen, D. J. Malvin, V. F. Buchwald and J. T. Wasson, *Geochimica et. Cosmochimica Acta*, 1984, **48**, 805-813.

Name	Type	Place found	Origin
Chinga	IVB-an	Tyva Republic, Russia	CSGM IGM SB RAS[1]
Sikhote-Alin	IIB	Primorsky Krai, Russia	CSGM IGM SB RAS[1]
Cheder	IID	Tyva Republic, Russia	CSGM IGM SB RAS[1]
Elga	IIE	Sakha (Yakutia) Republic, Russia	CSGM IGM SB RAS[1]
Darinskoe	IIC	Uralsk, Kazakhstan	CSGM IGM SB RAS[1]
Canyon-Diablo	IAB-MG	Arizona, USA	Specimen 1: RBINS[2]
			Specimen 2: Ordered from meteorite market (Alaska, USA)
Miles	IIE	Queensland, Australia	RBINS[2]

Table 1. List of the iron meteorites studied. [1] - CSGM IGM SB RAS stands for Central Siberian Geological Museum, V.S. Sobolev Institute of Geology and Mineralogy Siberian Branch of Russian Academy of Sciences, Novosibirsk, Russia. [2] – RBINS stands for Royal Belgian Institute of Natural Sciences.

		Bulk LA-ICP-MS	Mapping LA-ICP-MS	PN-ICP-MS
Element 2 ICP-MS unit				
Plasma power		850 W	850 W	1200 W
Sample introduction		LA	LA	Quartz cyclonic spray chamber and Micromist concentric nebulizer, 350 µl·min^{-1} uptake
Sampler Cone		Ni; 1.1 mm aperture diameter		
Skimmer cone		Ni; H-type; 0.8 mm aperture diameter		
Argon gas flow rates	Cool	16.00 L·min^{-1}	16.00 L·min^{-1}	16.00 L·min^{-1}
	Auxiliary	1.20 L·min^{-1}	1.20 L·min^{-1}	1.20 L·min^{-1}
	Carrier	1.573 L·min^{-1}	1.573 L·min^{-1}	0.930 L·min^{-1}
Resolution		Low, Medium (M/ΔM=300, 4000)	Low (M/ΔM=300)	Medium, High (M/ΔM=4000, 10000)
Nuclides monitored		Low resolution: ^{51}V, ^{52}Cr, ^{55}Mn, ^{59}Co, ^{60}Ni, ^{63}Cu, ^{66}Zn, ^{69}Ga, ^{74}Ge, ^{75}As, ^{90}Zr, ^{95}Mo, ^{99,101}Ru, ^{103}Rh, ^{105}Pd, ^{115}In, ^{118}Sn, ^{121}Sb, ^{178}Hf, ^{182}W, ^{185}Re, ^{190}Os, ^{193}Ir, ^{195}Pt, ^{197}Au, ^{208}Pb. Medium resolution: ^{74}Ge, ^{75}As, ^{95}Mo, ^{99}Ru, ^{101}Ru, ^{103}Rh.	Low resolution: ^{57}Fe, ^{59}Co, ^{60}Ni, ^{69}Ga, ^{74}Ge, ^{95}Mo, ^{99,101}Ru, ^{103}Rh, ^{105}Pd, ^{182}W, ^{185}Re, ^{190}Os, ^{193}Ir, ^{195}Pt, ^{197}Au.	Medium resolution: ^{51}V, ^{52}Cr, ^{55}Mn, ^{59}Co, ^{60}Ni, ^{63}Cu, ^{66}Zn, ^{69}Ga, ^{74}Ge, ^{75}As, ^{85}Rb, ^{90}Zr, ^{95}Mo, ^{99,101}Ru, ^{103}Rh, ^{105}Pd, ^{115}In, ^{128}Sn, ^{121}Sb, ^{178}Hf, ^{182}W, ^{185}Re, ^{190}Os, ^{193}Ir, ^{195}Pt, ^{197}Au, ^{208}Pb, ^{209}Bi. High resolution: ^{75}As, ^{85}Rb, ^{209}Bi.
Runs and passes		50 x 1	175 x 1 (adjusted to the time interval in which a 2800 µm line is ablated)	9 x 3
Samples per peak		10	10	20
Time per pass		2.573 (LR) +1.472 (MR) s	2.014 s	8.613 (MR) +1.307 (HR) s
New Wave Research UP-213 LA-system				
Laser wavelength		213 nm	213 nm	-
Laser pulse duration		3-5 ns	3-5 ns	-
Laser beam diameter		100 µm	40 µm	-
Laser fluence		7-8 J·cm^{-2}	7-8 J·cm^{-2}	-
Translation speed		10 µm·s^{-1}	10 µm·s^{-1}	-
Total area ablated		0.54 mm^2	7.84 mm^2	-

Table 2. ICP-MS and LA instrument settings used for ICP-MS analyses of iron meteorites.

Plasma power		1200 W
Sample introduction		Quartz cyclonic spray chamber and Micromist concentric nebulizer, 350 µl·min^{-1}
Sampler cone		Ni; 1.1 mm aperture diameter
Skimmer cone		Ni; H-type; 0.8 mm aperture diameter
Argon gas flow rates	Cool	15,00 L·min^{-1}
	Auxiliary	0,75 L·min^{-1}
	Nebulizer	0,924 L·min^{-1}
Resolution		Low (M/ΔM=300)
Nuclides monitored		^{99,101}Ru, ^{105,108}Pd, ^{191,193}Ir, ^{194,195}Pt
Detection mode		Triple
Scan type		E-scan
Samples per peak		30
Settling time		0,001 s
Runs and passes		15 x 15
Segment duration		0,180 s

Table 3. Instrument settings of the ELEMENT XR ICP-MS unit used for ID-PN-ICP-MS analysis of iron meteorites.

	Ni	Ir	Fe	Co	Ga	Ge	Ru	Rh	Pd	Os	Pt	Au	Re	W
Ni	1													
Ir	-0.17	1												
Fe	-1.00	0.17	1											
Co	**-0.52**	0.30	**0.52**	1										
Ga	-0.28	**0.50**	0.28	0.36	1									
Ge	**-0.50**	**0.62**	**0.50**	**0.55**	**0.63**	1								
Ru	0.05	**0.65**	-0.05	0.15	0.38	0.38	1							
Rh	-0.05	**0.69**	0.05	0.20	**0.41**	**0.45**	**0.62**	1						
Pd	0.13	0.34	-0.13	-0.04	0.17	0.06	0.36	0.33	1					
Os	-0.15	**0.82**	0.15	0.27	**0.48**	**0.55**	**0.61**	**0.65**	0.37	1				
Pt	-0.16	**0.86**	0.16	0.28	**0.47**	**0.55**	**0.63**	**0.67**	0.36	**0.80**	1			
Au	-0.09	**0.42**	0.09	0.12	0.26	0.25	0.29	0.32	0.27	**0.42**	**0.44**	1		
Re	-0.09	0.35	0.09	0.12	0.17	0.24	0.23	0.28	0.15	0.34	0.34	0.16	1	
W	-0.12	**0.47**	0.12	0.14	0.29	0.29	0.32	0.38	0.24	**0.45**	**0.46**	0.30	0.22	1

Table 4. Matrix of Pearson's product-moment correlation coefficients calculated from the LA-ICP-MS spatially resolved quantitative data for the Darinskoe IIC iron meteorite.

	LoD, 3σ			DARINSKOE				SIKHOTE-ALIN			
	I	II	III	I	II	III	IV	I	II	III	IV
Co, %	$8\cdot10^{-4}$	$1\cdot10^{-5}$	-	0.592±0.042	0.679±0.035	-	-	0.550±0.077	0.482±0.002	-	0.528
Ni, %	10^{-1}	$3\cdot10^{-4}$	-	11.4±1.3[4]	12.66±0.66	-	10.09	-	5.585±0.031	-	5.858
Cu, μg/g	10^{2}	$3\cdot10^{-1}$	-	146.9±3.4[1]	279±36	-	-	154.9±3.42	114.3±4.8	-	108
Ga, μg/g	10	$2\cdot10^{-2}$	-	44.0±9.5[4]	39.8±2.2	-	31	82.7±5.4	56.6±1.1	-	53
Ge, μg/g	10	$6\cdot10^{-1}$	-	90±19[4]	34.8±1.2	-	75	142±24	141.7±4.3	-	153
As, μg/g	6	7	-	5.6±1.9[5]	BDL<7	-	-	11.72±0.08[5]	BDL<7	-	9.0
Mo, μg/g	10	$3\cdot10^{-1}$	-	18.3±2.5[2]	8.60±0.16	-	-	10.6±4.2[2]	6.05±0.20	-	6.8
Ru, μg/g	2	$2\cdot10^{-1}$	$4\cdot10^{-3}$	25.1±2.5[4]	7.70±0.20	11.08±0.32	-	4.43±0.83	3.43±0.10	3.98±0.35	3.6
Rh, μg/g	$4\cdot10^{-1}$	$2\cdot10^{-1}$	-	1.61±0.33[4]	1.566±0.031	-	-	3.25±0.43	1.651±0.032	-	1.99
Pd, μg/g	4	$4\cdot10^{-2}$	$2\cdot10^{-3}$	2.87±0.59[4]	2.341±0.066	5.72±0.29	-	4.84±0.64[4]	1.864±0.060	3.87±0.27	2.81
W, μg/g	$2\cdot10^{-1}$	$5\cdot10^{-1}$	-	3.37±0.71[4]	0.938±0.022	-	-	1.23±0.06	0.655±0.019	-	0.76
Re, μg/g	10^{-1}	$6\cdot10^{-3}$	$3\cdot10^{-4}$	1.01±0.19[4]	1.30±0.11	1.204±0.042	-	BDL<10^{-1}	BDL<$6\cdot10^{-3}$	$(3.15\pm0.26)\cdot10^{-3}$	$3\cdot10^{-3}$
Ir, μg/g	$4\cdot10^{-1}$	$9\cdot10^{-3}$	$4\cdot10^{-3}$	12.8±2.3[4]	12.1±1.2	11.103±0.073	9.2	BDL<$4\cdot10^{-1}$	$(7.3\pm1.6)\cdot10^{-2}$	$(1.790\pm0.026)\cdot10^{-2}$	$1.9\cdot10^{-2}$
Pt, μg/g	3	$2\cdot10^{-2}$	$4\cdot10^{-3}$	13.5±2.6[4]	15.0±1.2	17.4±1.1	-	8.90±0.63	6.56±0.24	5.44±0.19	4.7
Au, μg/g	$4\cdot10^{-1}$	$6\cdot10^{-1}$	$3\cdot10^{-3}$	0.61±0.15[4]	0.639±0.073	0.902±0.014	-	1.68±0.15	1.23±0.047	1.052±0.030	1.028
Pb, μg/g	10^{-1}	$6\cdot10^{-2}$	-	BDL<0.1	0.091±0.012	-	-	0.148±0.014	0.095±0.025	-	-

Table 5. Concentration of 16 elements in 2 iron meteorites, μg/g: I- determined by LA-ICP-MS, II – determined by pneumatic nebulization ICP-MS, III- determined after anion exchange isolation by ID-PN-ICP-MS (Ru, Pd, Ir, Pt) and PN-ICP-MS (Au, Re), IV – reference values.

	ELGA				CHINGA				MILES		CHEDER	
	I	II	III	IV	I	II	III	IV	I	IV	I	IV
Co, %	0.415±0.012	0.471±0.002	-	0.456	0.248±0.003	0.595±0.016	-	0.577	0.653±0.018	0.44	0.6781±0.0	0.550
Ni, %	-	8.226±0.030	-	8.115	-	16.22±0.14	-	16.60	-	7.96	-	10.50
Cu, µg/g	211±30	183.1±9.8	-	194	BDL<100	18.0±1.7	-	-	BDL<100	182	495±86	539
Ga, µg/g	23.6±2.8	23.71±0.74	-	23	BDL<3	BDL<2	-	0.185	29.1±0.16	26.6	136±24	131
Ge, µg/g	67±2	36.2±1.2	-	72	BDL<10	BDL<2	-	0.082	91±10	-	154±47	148
As, µg/g	9.3±3.1[5]	BDL <7	-	10.3	BDL<5[5]	BDL <7	-	1.76	10.4±4.3	9.52	19.85±0.64	16.1
Mo, µg/g	8.2±3.3[2]	8.06±0.19	-	-	5.3±1.4[2]	5.76±0.28	-	7.4	BDL<10	-	13.1±3.6[2]	15.4
Ru, µg/g	5.95±0.09	5.75±0.17	6.23±0.30	-	3.70±0.25	4.58±0.15	6.30±0.17	7.9	3.7±1.4	-	36.0±0.1	28.3
Rh, µg/g	1.775±0.072	1.466±0.051	-	-	1.54±0.52	1.47±0.15	-	2.4	2.50±0.20	-	1.96±0.27	1.7
Pd, µg/g	4.23±0.91[3]	3.42±0.10	6.47±0.63	-	8.5±2.1[3]	6.05±0.23	10.17±0.25	7.9	BDL<4	-	BDL <4	2.0
W, µg/g	0.96±0.18	0.953±0.020	-	1.19	0.616±0.018	BDL <0.5	-	0.61	0.86±0.11	0.86	4.03±0.75	-
Re, µg/g	0.41±0.14	0.376±0.017	0.327±0.014	0.390	0.95±0.12	0.927±0.058	1.143±0.014	0.96	0.11±0.06	0.10	1.30±0.76	1.5
Ir, µg/g	3.11±0.38	4.76±0.23	2.69±0.013	4.00	2.55±0.16	2.65±0.51	3.45±0.016	3.90	1.14±0.20	1.12	14.4±1.5	19.0
Pt, µg/g	10.20±0.13	14.52±0.59	10.20±0.17	-	6.98±0.43	5.74±0.92	9.09±0.31	9.6	6.0±1.7	4.6	17.8±2.4	15.0
Au, µg/g	1.25±0.12	1.711±0.080	1.298±0.031	1.18	0.670±0.043	BDL <0.6	0.544±0.010	0.510	2.18±0.06	1.13	0.86±0.43	-
Pb, µg/g	BDL<0.1	0.121±0.015	-	-	0.141±0.015	BDL <0.06	-	-	0.47±0.03	-	0.570±0.06	-

Table 5. Concentration of 16 elements in 4 iron meteorites, µg/g: I- determined by LA-ICP-MS, II – determined by pneumatic nebulization ICP-MS, III- determined after anion exchange by ID-PN-ICP-MS (Ru, Pd, Ir, Pt) and PN-ICP-MS (Au, Re), IV – reference values.

[1] High inhomogeneity of Cu was found in Darinskoe at the level of the beam size used. Cu concentration results of 122 µg/g, 198 µg/g and 569 µg/g were found in different regions of the laser ablation line.

[2] LA-ICP-MS data obtained using UP193HE ArF* LA-unit coupled to XSeries II ICP-MS instrument for Mo, because the Element2 instrument suffered from severe Mo memory effects. NBS1286 CRM was used as external standard for quantification.

[3] LA-ICP-MS data obtained using UP193HE ArF* LA-unit coupled to XSeries II ICP-MS instrument for Pd, because the Element2 instrument suffered from severe Pd memory effects.

[4] Value obtained via mapping LA-ICP-MS.

[5] LA-ICP-MS data obtained using UP193HE ArF* LA-unit coupled to XSeries II ICP-MS instrument for As.

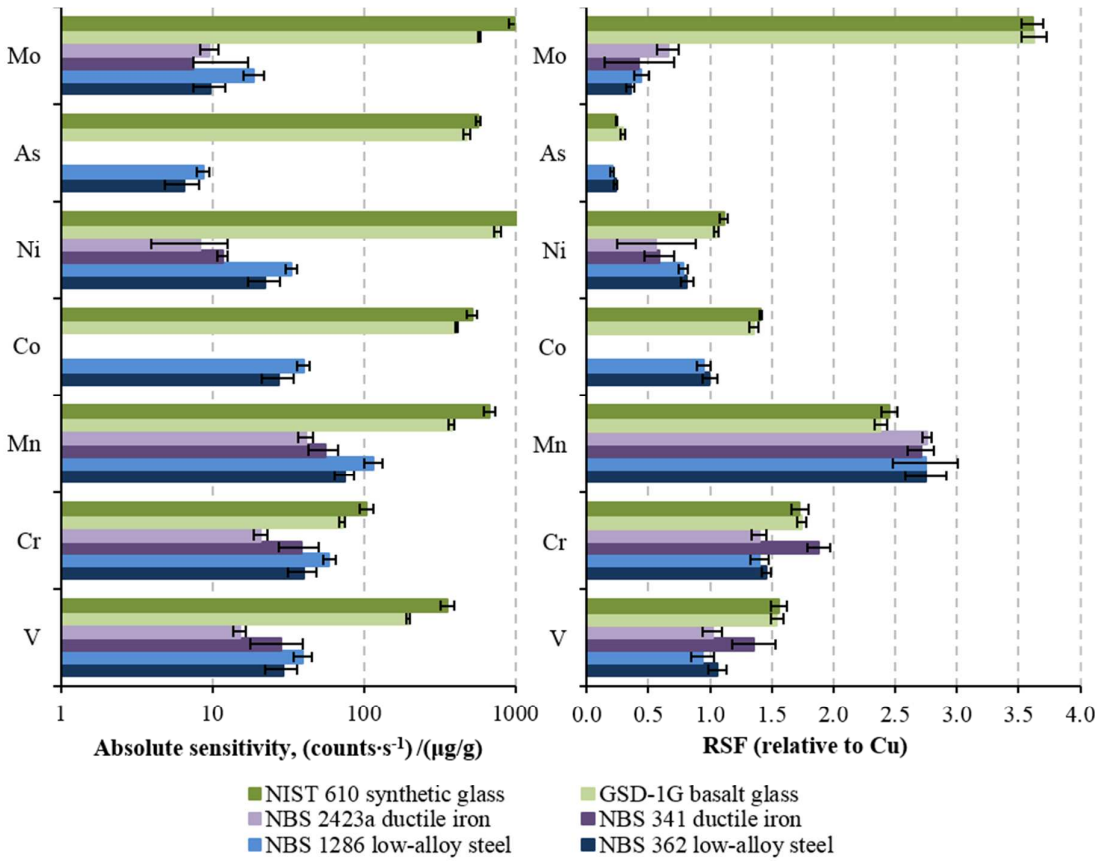

Fig. 1 Matrix effects in LA-ICP-MS analysis of iron and glass matrix.

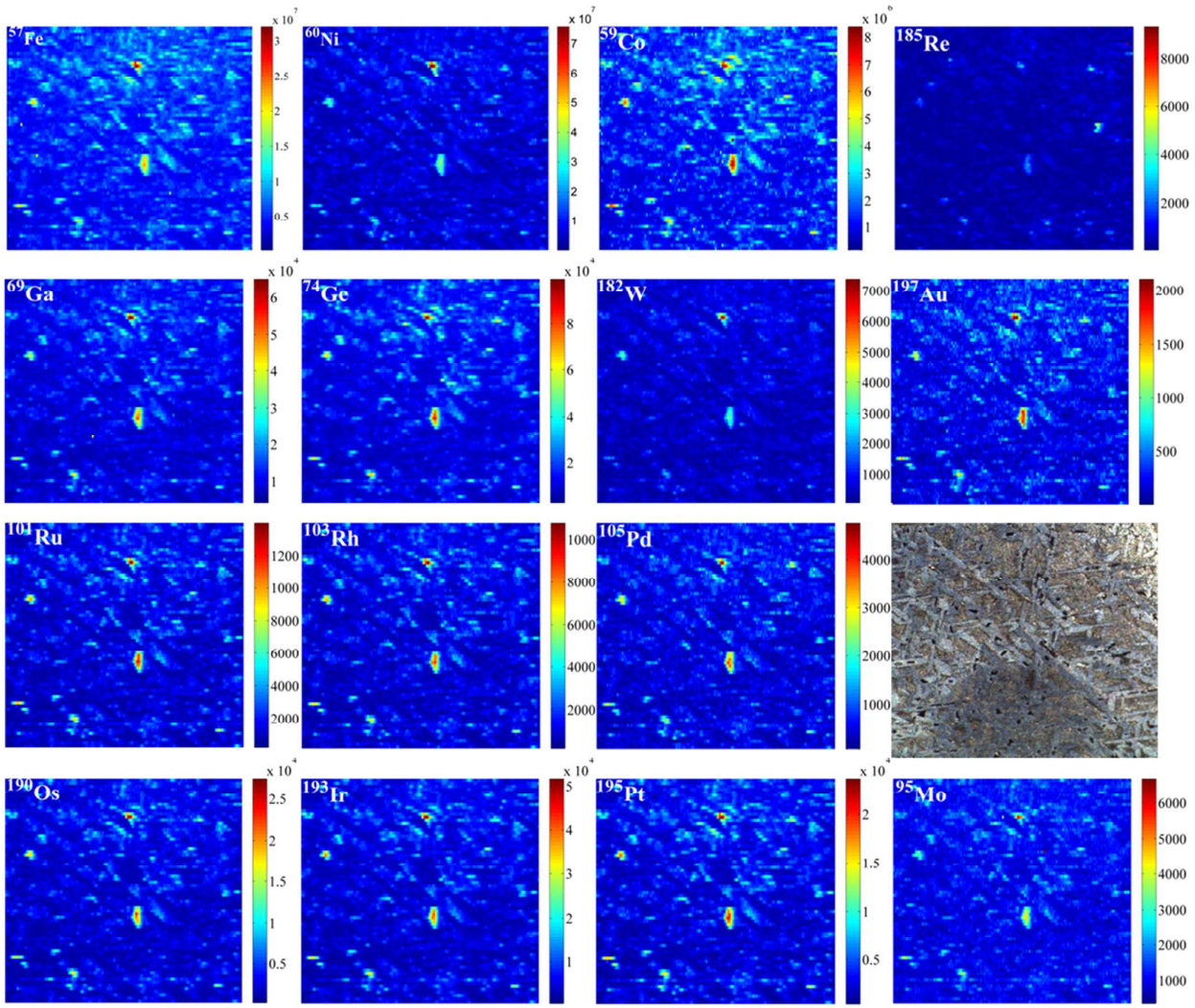

Fig. 2 Intensity distribution maps for 15 elements in a thick section of Darinskoe IIC iron meteorite, counts per second. Each map is composed of 72 lines of 40 μm width. The width of the image is 2800 μm.

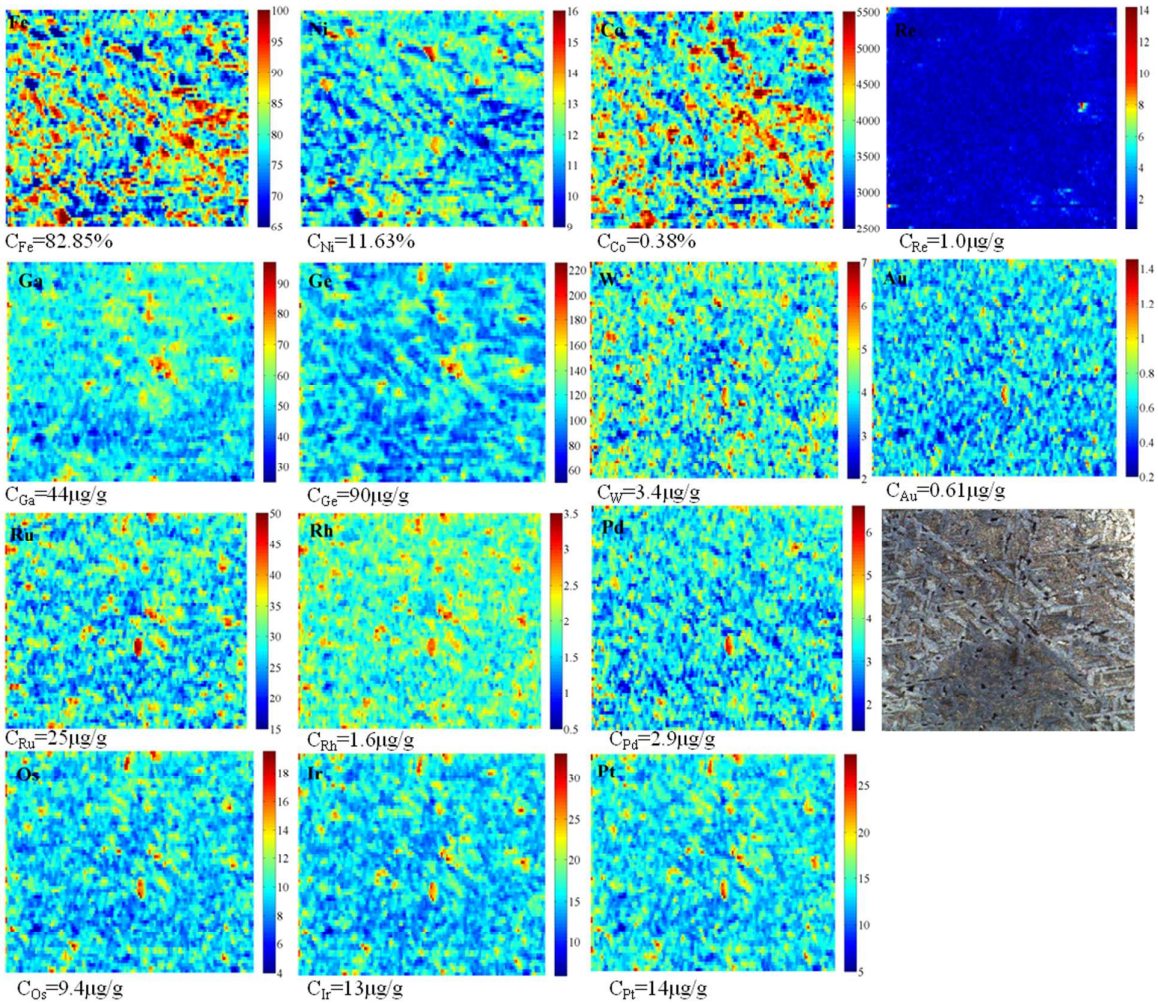

Fig. 3 Concentration distribution maps for 14 elements in a thick section of Darinskoe IIC iron meteorite, Fe, Ni – weight %, other elements –µg/g. The deviation from 100% stems from calculation of the concentration relative to external standard. The Mo distribution is not shown because of its low occurrence in the external standard. The width of the image is 2800 µm.

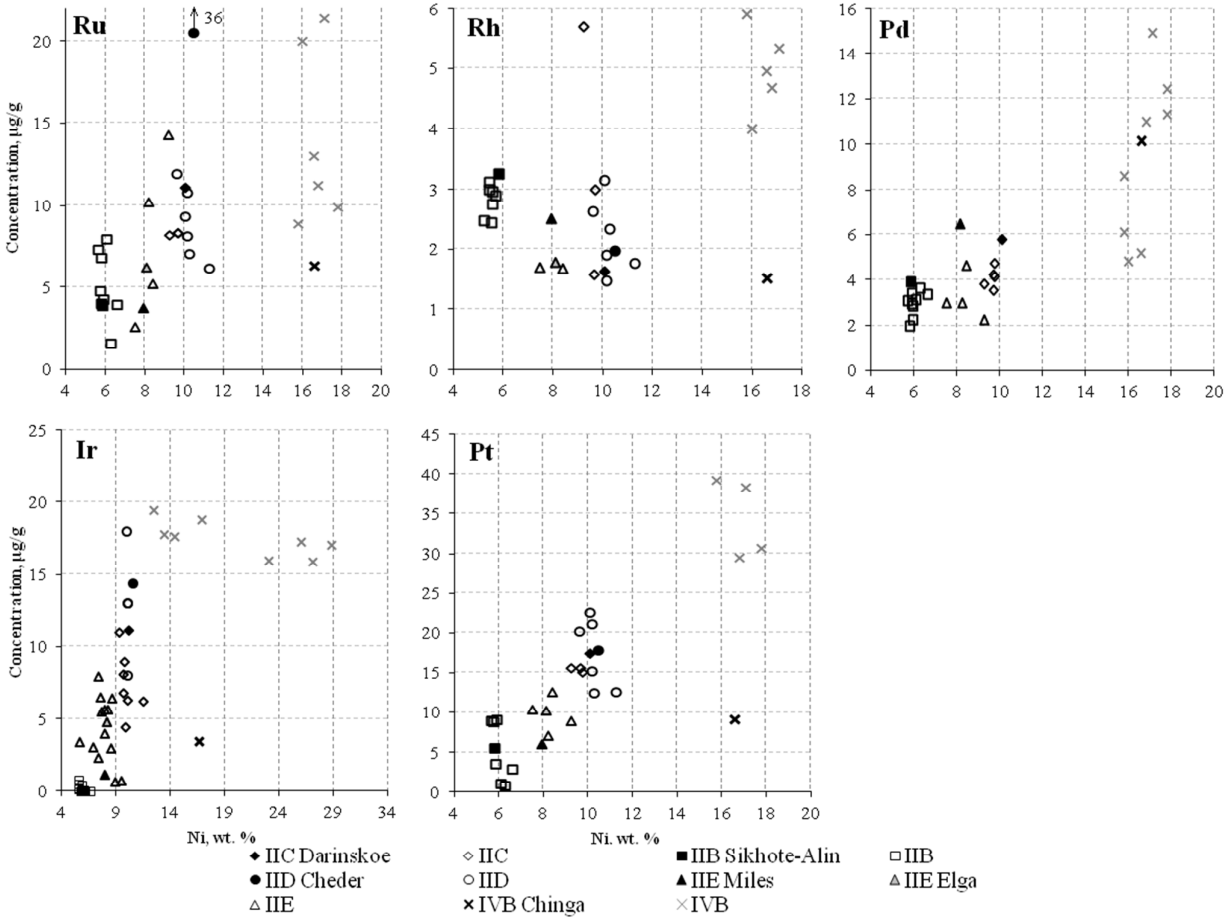

Fig. 4 Comparison of the PGE concentrations obtained with literature data for other iron meteorites of the same group. Filled symbols – this work, open symbols – literature data.

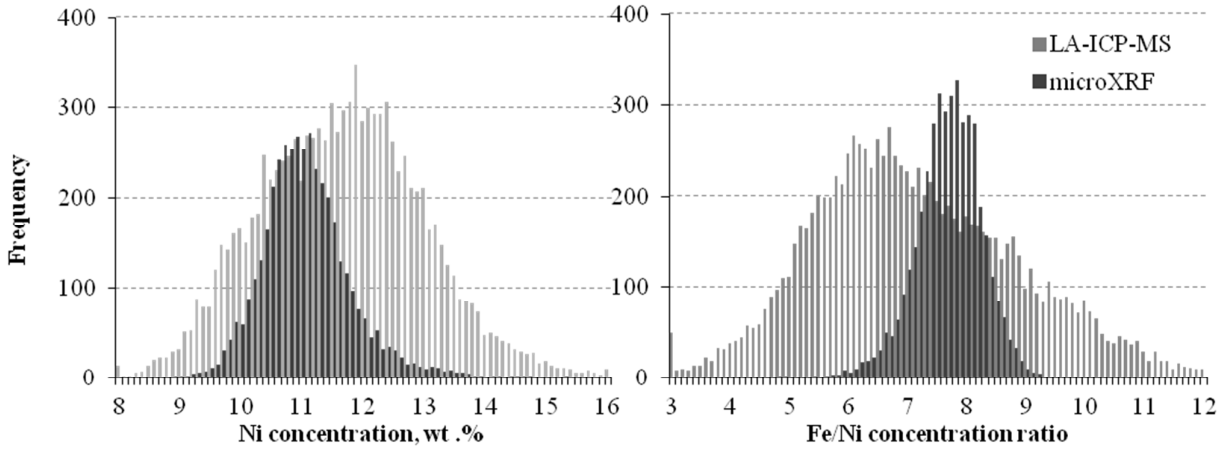

Fig. 5 Comparison of the distribution of the Ni concentrations and Fe/Ni ratios for a polished section of Darinskoe meteorite. Average Ni concentrations are 11.6 and 11.0% for mapping LA-ICP-MS and micro-XRF, respectively. Average Fe/Ni ratios are 7.1 and 7.6.

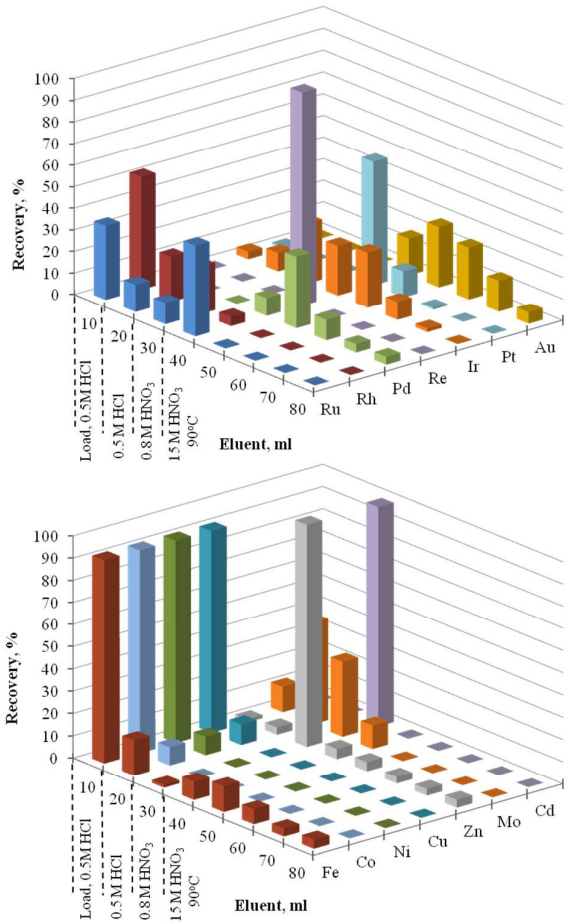

Fig. 6 Elution profile obtained using the anion exchange procedure. Recoveries were measured in each fraction via PN-ICP-MS.

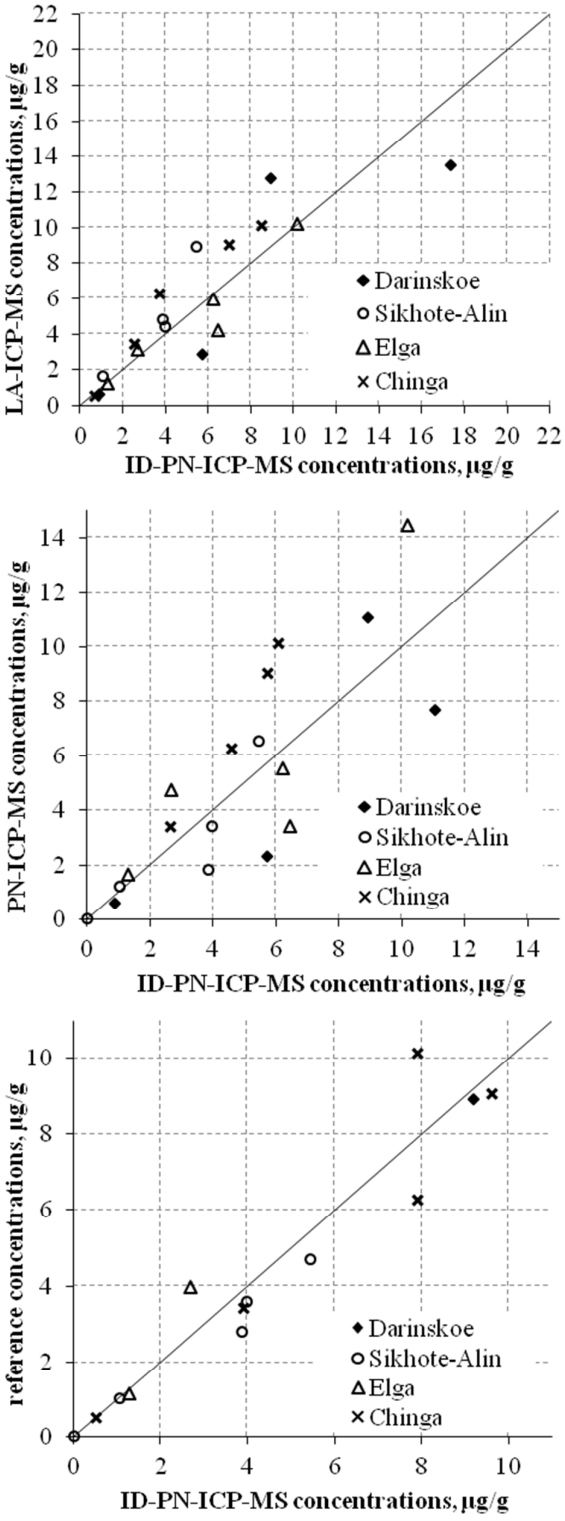

Fig. 7 Correlation of the concentrations of the PGE, Re and Au in 4 iron meteorites determined by different methods with ID-PN-ICP-MS (this work) with A. LA-ICP-MS data, B. PN-ICP-MS data, C. reference values.

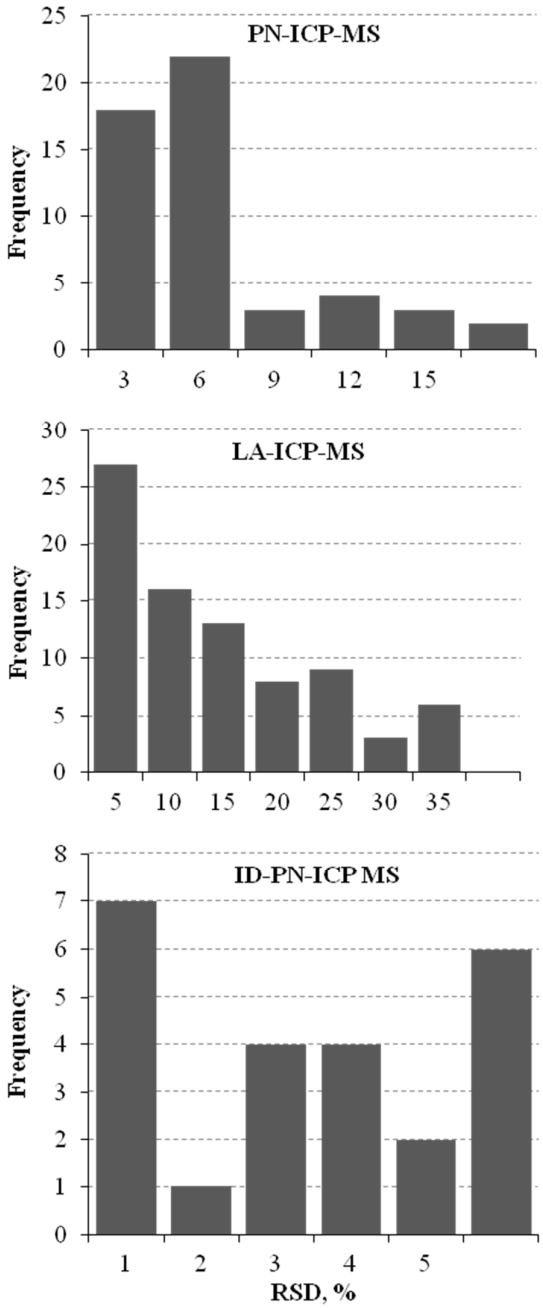

Fig. 8 Distribution of RSDs for PN-ICP-MS, LA-ICP-MS and ID-PN-ICP-MS.

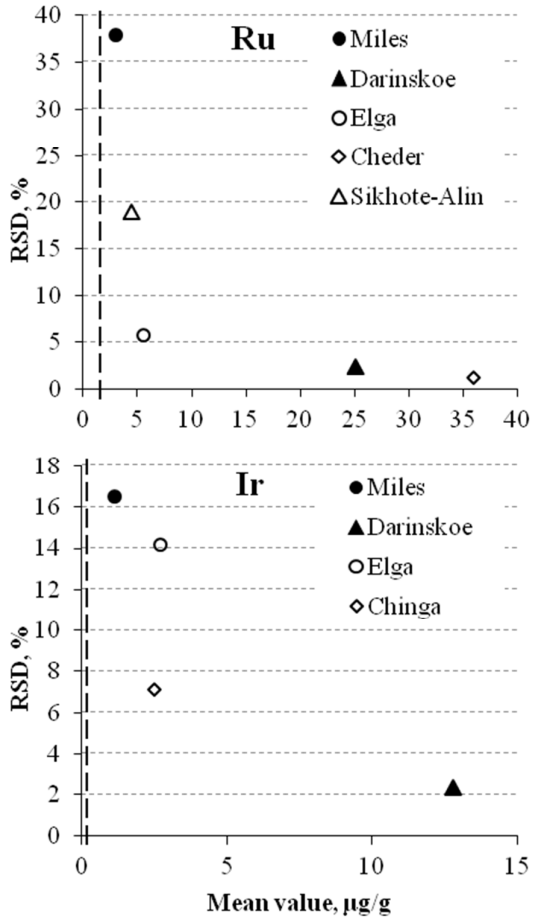

Fig. 9 Effect of the concentration level on the relative standard deviation in LA-ICP-MS analysis. The dashed line indicates the LoD (3s).